

Dynamical virial masses of Lyman–break galaxy haloes at $z = 3$

Stephen J. Weatherley* and Stephen J. Warren

Astrophysics Group, Blackett Laboratory, Imperial College London, Prince Consort Road, London SW7 2BW, UK

Accepted 0000 January 00. Received 0000 January 00; in original form 0000 January 00

ABSTRACT

We improve on our earlier dynamical estimate of the virial masses of the haloes of Lyman-break galaxies (LBGs) at redshift $z = 3$ by accounting for the effects of seeing, slit width, and observational uncertainties. From an analysis of the small number of available rotation curves for LBGs we determine a relation $V_{c7} = (1.9 \pm 0.2)\sigma$ between circular velocity at a radius of 7 kpc, V_{c7} , and central line velocity width, σ . We use this relation to transform the measured velocity widths of 32 LBGs to the distribution of circular velocities, V_{c7} , for the population of LBGs brighter than $\mathcal{R} = 25.5$. We compare this distribution against the predicted distribution for the ‘massive–halo’ model in which LBGs pinpoint all of the highest mass dark matter haloes at that epoch. The observed LBG circular velocities are smaller than the predicted circular velocities by a factor $> 1.4 \pm 0.15$. This is a lower limit as we have ignored any increase of circular velocity caused by baryonic dissipation. The massive–halo model predicts a median halo virial mass of $10^{12.3}M_{\odot}$, and a small spread of circular velocities, V_{c7} . Our median estimated dynamical mass is $< 10^{11.6 \pm 0.3}M_{\odot}$, which is significantly smaller; furthermore, the spread of our derived circular velocities is much larger than the massive–halo prediction. These results are consistent with a picture which leaves some of the most–massive haloes available for occupation by other populations which do not meet the LBG selection criteria. Our new dynamical mass limit is a factor three larger than our earlier estimate which neglected the effects of seeing and slit width. The median halo mass recently estimated by Adelberger et al. from the measured clustering of LBGs is $10^{11.86 \pm 0.3}M_{\odot}$. Our dynamical analysis appears to favour lower masses and to be more in line with the median mass predicted by the collisional starburst model of Somerville et al., which is $10^{11.3}M_{\odot}$.

Key words:

galaxies: kinematics and dynamics – galaxies: formation – galaxies: high redshift

1 INTRODUCTION

The development of the Lyman–break selection technique (Steidel & Hamilton, 1993) led to the first substantial samples of galaxies at high redshifts. There is now a wealth of observational data on this population, including optical and near-infrared photometry; optical and near-infrared spectroscopy; and measurement of their clustering properties (Steidel, Pettini & Hamilton, 1995; Shapley et al., 2001; Shapley et al., 2003; Pettini et al., 2001; Adelberger et al., 1998; Giavalisco & Dickinson, 2001). Nonetheless, the most fundamental quantity – the dark–matter halo virial mass, or equivalently the circular velocity at large radius – is poorly determined for Lyman–break galaxies (LBGs). This is be-

cause it requires observations in the very faint outer regions of galaxies of rest–frame optical emission lines, which are redshifted to the near–infrared where the night sky is bright. As a consequence only a handful of rotation curves, with low signal–to–noise and compromised by seeing, have been measured for LBGs. This paper is concerned with extracting the maximum useful information on the virial masses of the haloes of LBGs from the existing kinematic data. Throughout the paper the term LBG refers to galaxies at $z = 3$ identified by their spectral discontinuity at the Lyman–limit, that are brighter than $\mathcal{R} = 25.5$ (Adelberger et al., 1998).

Lacking high quality rotation curves, most of our knowledge of the virial masses of LBGs comes indirectly, from an interpretation of their clustering properties. The strong clustering measured in the counts–in–cells analysis of Adelberger et al. (1998) and in the correlation–function analysis

* Email : stephen.weatherley@imperial.ac.uk

of Giavalisco & Dickinson (2001), and the dependence of the correlation length on luminosity detected in the latter study, were interpreted as implying that LBGs are associated with dark matter haloes of high mass – consistent with a simple model in which LBGs pinpoint all the highest mass dark matter haloes at that epoch. We refer to this model as the ‘massive–halo’ model and use the results of the analysis by Mo, Mao & White (1999; hereafter MMW) as defining the model. Their figure 4 provides the predicted distribution of halo circular velocities at the virial radius, and yields a median halo virial mass of $10^{12.3}M_{\odot}$ for the LBG population. The massive–halo model leaves no room for other high–redshift populations, that do not meet the LBG criteria, to occupy the high–mass tail of the halo distribution, such as sub-mm galaxies (Smail, Ivison & Blain, 1997) and red galaxies (Franx et al., 2003). Adelberger et al. (2005) have recently measured the clustering of a new, larger, sample of LBGs: through comparison with n–body simulations they estimate a median halo mass of $10^{11.86\pm 0.3}M_{\odot}$. The best–fit value for the median mass is a factor three lower than in the massive–halo model, in which case not all of the most–massive haloes would be occupied by LBGs – leaving some space for other galaxy types.

Unfortunately the clustering results allow for more than one interpretation. As shown by Wechsler et al. (2001) an alternative model proposed by Somerville, Primack & Faber (2001; hereafter SPF), in which LBGs have lower masses but are temporarily brightened due to merger–induced star formation, predicts similarly strong clustering as the massive–halo model. In this picture the virial masses are an order of magnitude lower than in the massive–halo model, with median value of $10^{11.3}M_{\odot}$ (Primack, Wechsler & Somerville, 2003).

Finally, an indirect lower limit to the halo masses is provided by multiplying the estimated stellar masses of LBGs by the ratio of the cosmological matter density to the density in baryons (Ω_m/Ω_b). Taking the median value of the stellar mass estimated by Shapley et al. (2001), from fits to optical and near-infrared photometry, this provides a lower limit to the median halo virial mass of $10^{11.1}M_{\odot}$.

To summarise, current estimates of the median halo virial mass of LBGs at redshift $z = 3$, which are all indirect, cover a wide range, $10^{11.1}M_{\odot}$ to $10^{12.3}M_{\odot}$. Motivated by this large uncertainty, in an earlier paper (Weatherley & Warren, 2003; hereafter Paper I) we presented a simplified analysis of the kinematic data on LBGs, to estimate the halo virial masses. The Λ CDM paradigm for structure formation permits computation of the detailed properties of the dark matter yielding predictions of the masses of haloes, their mass profiles, and their assembly history (e.g. Lacey & Cole, 1993; Navarro, Frenk & White, 1997, hereafter NFW). Baryonic processes, including star formation and feedback, on the other hand are too complex to allow *ab initio* predictions of the distribution and state of the baryons within the haloes. Therefore the best tests of the Λ CDM paradigm will be those which measure the properties of the dark matter. Instead, at high redshift, we are largely limited to studies of luminous matter in the brightest central regions of galaxies, where the baryons dominate the mass budget. For example, in most cases the kinematic data on LBGs is limited to the measured line velocity widths. These data, on their own, are not useful for measuring halo masses; fortunately, in a

handful of cases spatially resolved data have been obtained, extending to projected radii of a few kpc.

Our dynamical analysis centred on these rotation velocities, V_r . In Paper I we collated the useful kinematic data on LBGs, selecting from the datasets of Pettini et al. (2001) and Erb et al. (2003), to define a sample of seven measured projected rotation velocities, V_r , as well as 32 velocity widths, characterised by the dispersion of the velocity profile σ . The galaxies for which rotation curves have been measured may not be representative of the LBG population: for example the luminosity profiles may be more extended than average. For this reason, a simple statistical analysis of the rotation velocities is not appropriate. Instead we were able to use the rotation velocities by making the assumption that the distribution of measured values of the dimensionless quantity V_r/σ are representative. We then connected the rotation velocities, the velocity widths, and the Λ CDM predictions through the assumption of a linear relation $V_{c7} = \alpha\sigma$, where V_{c7} is the circular velocity at a radius of 7kpc.¹ The procedure was, firstly, to determine an observed value of $\alpha(obs)$ which, accounting for random orientations and inclinations (over $\cos(i)$), explained the observed distribution of V_r/σ of the seven galaxies. We found that a value $\alpha(obs) = \sqrt{2}$ (motivated by the isothermal sphere model) provided a satisfactory fit. This value of $\alpha(obs)$ then converts the distribution of the 32 values of σ , assumed representative of the population, to the distribution of V_{c7} for LBGs. We compared this against the, larger, required value of $\alpha(req) = 2.6$ that would be needed to reconcile the measured distribution of σ with the distribution of V_{c7} predicted by the massive–halo model. The small value of $\alpha(obs)$ was inconsistent with the required value of $\alpha(req)$, implying halo virial masses an order of magnitude smaller than the predictions of the massive–halo model.

Our previous analysis made a number of simplifying assumptions. In computing $\alpha(obs)$ we took no account of the effect of atmospheric seeing, which would blur the light from the bright, baryon dominated centres of the galaxies to the faint outer parts, smoothing the transition from +ve to –ve velocity in the rotation curve, such that the rotation velocity would be underestimated. The data we analysed were taken in average conditions of 0.5 arcsec seeing, and the rotation velocities were measured at an average offset of 0.64 arcsec. Erb et al. (2004) give an indication of the importance of seeing: in 0.9 arcsec seeing they measured a rotation velocity approximately half that measured for the same LBG in 0.5 arcsec seeing. As discussed later, and illustrated in Figure 3, we find that the reduction in measured rotation velocity in 0.5 arcsec seeing is indeed significant. Another important effect not accounted for in Paper I is the variation of projected velocity across the finite width of the slit (0.76 arcsec or 1.00 arcsec). The influences of seeing; slit width; galaxy luminosity profile; galaxy orientation and inclination; the observational errors; and selection cuts all interact in a complex manner. In this paper we improve on our previous study

¹ Our notation is as follows: rotation velocity, V_r , refers to half the measured peak–to–peak velocity spread of a spatially resolved velocity profile (the observed quantity). Circular velocity, V_c , refers to the de–projected, true, circular velocity of the galaxy. Similarly, we use the symbol r for projected radius and R for de–projected radius.

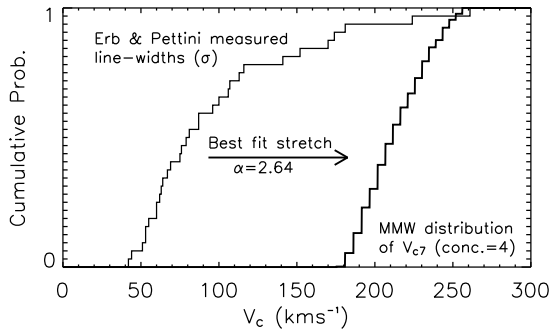


Figure 1. The cumulative PDF of the line velocity widths (Paper I, table 1) for LBGs compared with the distribution of V_{c7} predicted by the massive-halo model. A value $\alpha(req) = 2.64$ is required to reconcile the two curves.

by detailed modelling of these various effects and we investigate the sensitivity of our results to the assumptions made. We retain the formalism of the relation $V_{c7} = \alpha\sigma$ as the means of comparing theory and data. We employ a likelihood analysis, improving over the statistical analysis of Paper I. Throughout, we assume a standard, flat Λ CDM cosmology with $\Omega_\Lambda = 0.7$ and $H_0 = 70 \text{ km s}^{-1} \text{ Mpc}^{-1}$.

2 REVISED ANALYSIS

We follow the same principles as in our earlier analysis. The data analysed are the same seven rotation velocities, V_r , and 32 velocity widths, σ , summarised in Paper I. Below, we compare the σ distribution for the LBGs against the predicted distribution of V_{c7} for the massive-halo model to determine $\alpha(req)$. Secondly we reanalyse the seven measured rotation velocities and their associated values of σ , modelling the observational effects and selection cuts, as detailed below, to measure $\alpha(obs)$ – i.e. the value of α that gives the best fit to the distribution of V_r/σ for the seven galaxies. We then compute the probability of observing the seven values of V_r/σ assuming $\alpha = \alpha(req)$ – i.e. the probability that the massive-halo model fits the data.

At this point it is worth repeating, as emphasised in Paper I, that we make no assumption about the cause of the line broadening i.e. the relative contribution of pressure and rotational support to the velocity width. Our analysis is merely aimed at testing whether the observed seven values of the ratio V_r/σ are large enough to reconcile the σ distribution for LBGs with the massive-halo model.

2.1 Determining $\alpha(req)$

Figure 1 plots the cumulative PDF of the velocity widths (corrected for instrumental resolution) of the 32 LBGs (thick stepped line), taken from table 1, Paper I. For the seven galaxies with spatially resolved velocity profiles, σ was measured from the central line profile.

Also plotted in Figure 1 is the MMW prediction for the distribution of halo circular velocities at a radius of 7 kpc (thin stepped line). This was calculated starting with the distribution of halo velocities at the virial radius V_h from figure 4 of MMW. For the NFW profile, the conversion to circular velocity at radius R is

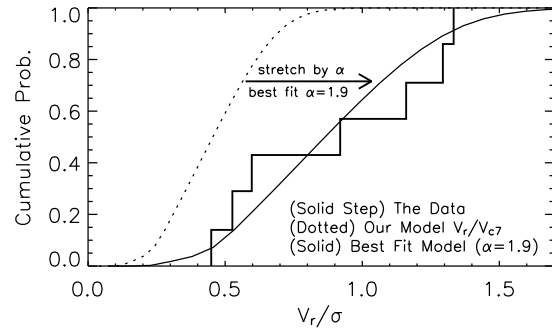


Figure 2. Cumulative PDF of the ratio V_r/σ for the seven galaxies of Pettini et al. and Erb et al. (table 2 in Paper I) shown as the solid stepped line. The dotted line shows the ratio of V_r/V_{c7} for our model galaxies, including errors and selection criteria. The solid smooth line shows the same curve, stretched by the best fit value of $\alpha = \alpha(obs)$, to match our model to the data.

$$\left(\frac{V_{cR}}{V_h}\right)^2 = \frac{1}{x} \frac{\ln(1+cx) - (cx)/(1+cx)}{\ln(1+c) - c/(1+c)},$$

where $x = R/R_h$. We use the relation $R_h = V_h/(10H(z))$ and we assume concentration $c = 4$. These are the circular velocities computed ignoring the effects of baryonic dissipation, which will raise the circular velocities. This increase is probably substantial but is difficult to predict reliably. The simple adiabatic contraction model (Mo, Mao & White 1998) indicates that the circular velocities V_{c7} could increase by a factor of about 1.5, but the detailed processes involved in baryonic contraction are poorly understood. There is both theoretical (El-Zant, Shlosman, & Hoffman 2001) and observational (Binney & Evans 2001) evidence to suggest that the increase may not be as great.

A stretch of the Erb and Pettini velocity widths of $\alpha(req) = 2.64$ gives the best fit to the predicted distribution of V_{c7} , as shown in Figure 1. It is noticeable that the predicted distribution of V_{c7} is rather narrow, compared to the broad distribution of σ . We consider this point again later.

2.2 Modelling observational effects and selection cuts to determine $\alpha(obs)$

The principle of measuring $\alpha(obs)$, accounting for observational effects and selection cuts, is illustrated in Figure 2, and is explained as follows. For galaxies of specified circular velocity radial profile, and luminosity radial profile, it is possible to predict the observed distribution of the ratio V_r/V_{c7} , for any given observing conditions – defined by the seeing, the slit width and the selection criteria. Since $\alpha = V_{c7}/\sigma$ we can stretch our model distribution of V_r/V_{c7} by a factor α to match the observed distribution of V_r/σ . This best fit stretch factor is $\alpha(obs)$. If the massive-halo model is correct $\alpha(obs)$ will be consistent with $\alpha(req)$. As regards the slit width, since two observational set-ups were used, with 0.76 arcsec (NIRSPEC) and 1.00 arcsec (ISAAC) slits, we model both cases, and weight the results by the fraction of observations with each slit. We now explain the modelling in detail.

The galaxy rotation curves are assumed to reflect the halo mass profile; therefore the galaxies are modelled as

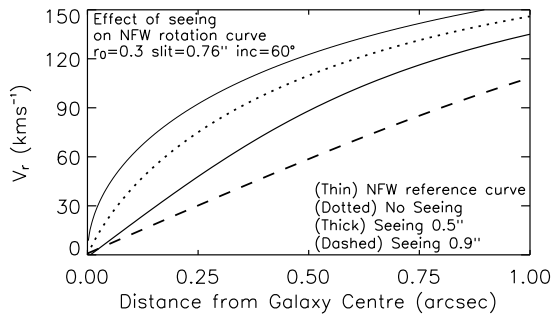


Figure 3. The effect of seeing on the measured rotation curve of a galaxy with halo velocity $V_h = 220 \text{ km s}^{-1}$ inclined at 60° to the sky, with major-axis aligned with the spectroscopic slit.

massless stellar discs of exponential luminosity profile – the choice of scale radius, R_0 , is discussed below. The distribution of galaxy circular velocity profiles is defined by the MMW halo circular velocity distribution, and the NFW mass profile, with concentration $c = 4$. No information on the inclination angles and position angles of the major axes were available at the time the spectra were acquired; therefore, we assume random inclination angles (over $\cos(i)$), and random orientations relative to the slit. The 2D luminosity-tagged velocity maps are convolved with the seeing, and the resulting luminosity-weighted velocity maps are averaged across the slit to produce luminosity-weighted observed rotation curves along the slit.

Example rotation curves for a galaxy with $V_h = 220 \text{ km s}^{-1}$, and inclination angle $i = 60^\circ$, oriented along the slit, are provided in Figure 3. The curves from top to bottom represent: i) the NFW circular velocity profile along the major axis; ii) the luminosity-weighted rotation curve obtained by averaging across the slit, before convolution by the seeing; iii) the observed rotation curve in 0.5 arcsec seeing; iv) the observed rotation curve in 0.9 arcsec seeing. At a position 0.75 arcsec along the slit, the measured rotation velocities are 0.85 and 0.62 of the NFW value on the major axis, for 0.5 arcsec and 0.9 arcsec seeing respectively.

To compare the model with the data we must reproduce the conditions by which the data were measured, as closely as possible. For a chosen scale radius R_0 , we measured the rotation velocity at the (deprojected) radius βR_0 , where the value of the constant β was chosen to reproduce the average projected radius of the measured rotation curves. For the rotation curve to be spatially resolved the projection of this distance on the slit had to be greater than some limiting value, which we took as $r_{lim} = 0.4 \text{ arcsec}$. If the simulation passes the spatial cut we add a velocity error drawn at random from an appropriate Gaussian distribution and then check if the observation meets the velocity cut, V_{min} . Rotation velocities were only recorded by Pettini et al. (2001) and Erb et al. (2003) if a velocity gradient was clearly visible, corresponding to a rotation velocity greater than twice the typical velocity error (Erb, private communication). Therefore, in our simulation, we disregard rotation velocities smaller than $V_{min} = 25 \text{ km s}^{-1}$ for the ISAAC data, and $V_{min} = 50 \text{ km s}^{-1}$ for the NIRSPEC data. We chose a nominal scale length $R_0 = 0.3 \text{ arcsec}$, and found that a value $\beta = 2.6$ reproduced the average projected radius of the seven measurements. This scale radius is about twice

as large as the typical value measured for LBGs (Marleau & Simard, 1998); nevertheless, given that rotation velocities were secured for only seven of the 32 LBGs considered here, it may be true that the light profiles of these seven galaxies are more extended on average.

In summary, our model is fully specified by the distribution of halo virial circular velocities from MMW and the following list of parameters (fiducial values in brackets):

- (i) σ_{atm} — the seeing with which we convolve the galaxy profiles (FWHM=0.5 arcsec, the quoted average value from Pettini et al. (2001), and Erb et al. (2003))
- (ii) c — the concentration parameter of the NFW halo profile (4)
- (iii) R_0 — scale-radius for the exponential light profile (0.3 arcsec); and the spatial cut r_{lim} (0.4 arcsec)
- (iv) V_{min} — the spectral cut (25 km s^{-1} for the ISAAC 1.00 arcsec slit and 50 km s^{-1} for the NIRSPEC 0.76 arcsec slit)

Later we assess how robust are the conclusions to variations in the chosen values of the above parameters.

3 RESULTS

3.1 Measuring $\alpha(obs)$

The results of the modelling are summarised in the curve of the expected distribution of V_r/V_{c7} plotted in Figure 2. Also plotted in the figure, as the stepped line, is the distribution of V_r/σ for the seven galaxies with recorded rotation velocities. Recall that $\alpha(obs)$ is the value by which the curve should be stretched to fit the stepped line, and that this should be consistent with $\alpha(req) = 2.64$ (Figure 1) if the massive-halo model is correct.

In Figure 4 (upper) we plot, as the solid curve, the likelihood of the data as a function of α , normalised to the peak. This is the posterior pdf (modulo a constant) for α adopting a uniform prior. The best fit, plotted as the stretched curve in Figure 2 is $\alpha(obs) = 1.9 \pm 0.2$. The probability of the data if α is as large or larger than $\alpha(req) = 2.64$ is $p = 0.013$. This means that the measured rotation velocities are too small to be consistent with the massive-halo model. Another way of visualising this result is to say that the rotation velocities imply a distribution of V_{c7} for LBGs which is the distribution of σ plotted in Figure 1 stretched by the factor $\alpha(obs) = 1.9$. The circular velocities are smaller than the predicted circular velocities for the massive-halo model by a factor 1.4 ± 0.15 .

3.2 Variation of model parameters

In this section we explore to what extent variation of the parameters of the model affects the conclusion that LBGs are significantly less massive than predicted by the massive-halo model.

- (i) We find that our results are not very sensitive to the exactly value of the seeing adopted. We repeated the entire analysis for values of 0.4 arcsec and 0.6 arcsec. The corresponding likelihood curves are shown in the top plot of Figure 4, and compared to the curve for the fiducial

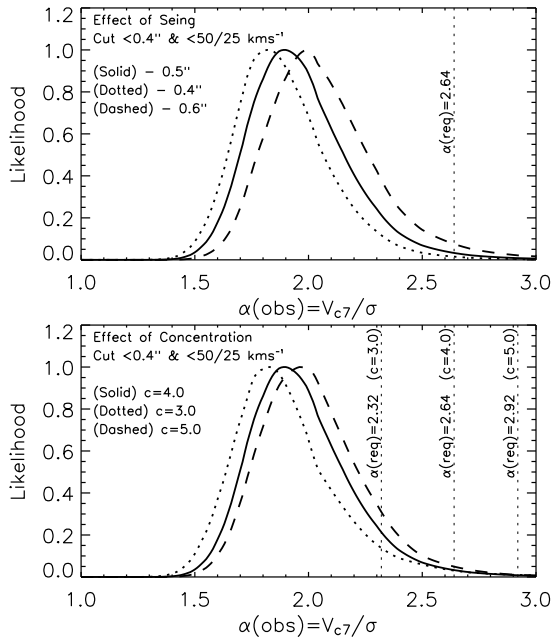


Figure 4. Likelihood plots (normalised to the peak) to show the effects of changing parameters in the model. The upper plot shows the effect of changing the atmospheric seeing, and the lower plot shows the effect of varying the concentration. All other parameters are kept fixed at the preferred values.

value of 0.5 arcsec. Over the range 0.4 – 0.6 arcsec the probability for the massive-halo model varies over the range $0.006 < p < 0.032$.

(ii) The lower plot shows the effect of varying the value of the concentration parameter c . Since the relation between V_{c7} and V_h depends on c , varying c changes not only the predicted rotation velocities but also the value of $\alpha(\text{req})$, as indicated on the plot. For the range of V_h specified by MMW a suitable range for the concentration parameter is $3 < c < 5$ (Bullock et al. 2001). For this range, the probability for the massive-halo model varies over the range $0.059 > p > 0.004$. Therefore, for a spread of values of c within the quoted range, the probability for the massive-halo model remains low.

(iii) The results are rather insensitive to small variations of the exponential scale radius, R_0 , and the spatial cut r_{lim} . This is because for variations in either parameter we have to adjust the parameter β such that the average projected radius at which the rotation velocity is measured matches that of the data. We confirmed that for smaller R_0 the measured $\alpha(\text{obs})$ is slightly higher, and *vice versa*. This is as expected because for smaller R_0 the light is more concentrated, so after convolution with the seeing the luminosity-weighted rotation velocity at any radius receives proportionally more light originating at smaller radius, where the rotation velocity is lower.

(iv) We also checked the sensitivity of the result to the value of the spectral cut V_{min} . Our analysis uses the spectral cuts applied to the data $V_{min} = 50 \text{ km s}^{-1}$ and $V_{min} = 25 \text{ km s}^{-1}$ for the NIRSPEC and ISAAC datasets respectively, and we have taken these at face value. Nevertheless it is interesting to check how the conclusions would have differed, had different cuts been applied. Higher cuts make

little difference, but lower cuts raise the likelihood of high values of α . For example had the same distribution of V_r/σ been observed for cuts as low as $V_{min} = 30 \text{ km s}^{-1}$ and $V_{min} = 15 \text{ km s}^{-1}$, for the NIRSPEC and ISAAC datasets, the data would be consistent with the massive-halo model, with $p = 0.15$. This may be understood by reference to Figure 2. Higher values of V_{min} raise the low-end cut off of the predicted curve of V_r/σ . High values of α are ruled out once the tail passes the first point on the stepped line. Lowering the cuts extends the tail of the curve to smaller values of V_r/σ , so that larger values of α are permitted. This illustrates the importance of specifying well-defined selection criteria.

4 DISCUSSION

To summarise the previous section, we have improved on our earlier dynamical estimate of the virial masses of the haloes of LBGs at redshift $z = 3$, by accounting for the effects of seeing, slit width, and observational uncertainties. From an analysis of the small number of available rotation curves for LBGs we determined a relation $V_{c7} = (1.9 \pm 0.2)\sigma$. We used this to transform the measured velocity widths of 32 LBGs to the distribution of circular velocities V_{c7} . We compared this distribution against the predicted distribution for V_{c7} for the massive-halo model. The LBG circular velocities are too small by a factor 1.4 ± 0.15 . As noted earlier, our analysis does not account for the increase in the circular velocity of the galaxies due to baryonic dissipation, so the quoted factor is a lower limit. With this in mind we can compute an upper limit to the median dynamical halo virial mass, by taking the median value of σ , and multiplying by 1.9 to convert to V_{c7} . Selecting an appropriate value of c , our median estimated dynamical halo mass is $< 10^{11.6 \pm 0.3} M_\odot$. Our new dynamical mass limit is a factor 3 larger than our earlier estimate (Paper I) which neglected the effects of seeing and slit width. Our dynamical mass limit is inconsistent with the value of $10^{12.3} M_\odot$ predicted by the massive-halo model. The broad spread in measured velocity widths (Figure 1), which translates to a broad spread in inferred V_{c7} is further evidence against the massive-halo model, which predicts a narrow spread in V_{c7} . A consistent picture is one in which LBGs inhabit only a fraction of the most-massive haloes. In this case the average mass will be lower and the range of masses will be larger. This conclusion finds some support in the recent clustering analysis of Adelberger et al. (2005): by matching the clustering strength, and space density to the corresponding quantities for haloes in an n -body simulation they derive a median halo mass of $10^{11.86 \pm 0.3} M_\odot$. Our analysis suggests lower masses still. Our result appears to be more consistent with the predicted masses of the collisional starburst model of SPF, which has a median halo mass of $10^{11.3} M_\odot$. The picture that emerges is one which leaves some of the most-massive haloes available for occupation by other populations which do not meet the LBG selection criteria.

These conclusions rest on the analysis of a small number of rotation curves of low signal-to-noise, without the benefit of complementary high-resolution imaging. Recently Erb et al. (2004) have questioned whether the majority of LBGs are dynamically relaxed, which would undermine the basis

of our calculation. In an attempt to maximise the chances of measuring rotation, they used HST imaging of a sample of galaxies at $z \sim 2$ to select the fraction with morphologies consistent with the expectation for edge-on disks. They obtained H α spectra for nine of their sample, with the slit aligned along the major axis. Contrary to expectation, rotation velocities were secured for only two of the galaxies. They proposed that these results could be explained if some of the elongated galaxies are in fact merging sub-units, rather than relaxed edge-on disks. It is worth noting, nevertheless, that the majority of these observations were undertaken in typical seeing of 0.8 arcsec, somewhat worse than for the data analysed here. Of the nine galaxies selected as elongated, in six cases the (deconvolved) extent of the H α emission is smaller than the seeing, which would make it difficult to detect rotation. Of the three cases where the H α emission is more extended than the seeing, rotation velocities were secured for two. This analysis further underscores the desirability of high-spatial resolution 2D spectroscopy, to remove some of these uncertainties of interpretation. In the meantime, our goal in this paper has been to maximise the useful information on the dynamical virial masses of the haloes of LBGs from existing kinematic data.

ACKNOWLEDGMENTS

We thank Dawn Erb and Max Pettini for their helpful comments regarding their data, and their constructive criticism of Paper I. We are grateful to the referee for comments which helped clarify this manuscript. SJW[1] also thanks Thomas Babbedge for his comments on previous drafts of this manuscript.

REFERENCES

- Adelberger K. L., Steidel C. C., Giavalisco M., Dickinson M. E., Pettini M., Kellogg M., 1998, ApJ, 505, 18
- Adelberger K. L., Steidel C. C., Pettini M., Shapley A. E., Reddy N. A. Erb D. K., 2005, ApJ, 619, 697
- Binney J. J., Evans N. W., 2001, MNRAS, 327, 27
- Bullock J.S., Kolatt T.S., Sigad Y., Somerville R.S., Kravtsov A.V., Klypin A.A., Primack J.R., Dekel A., 2001, MNRAS, 321, 559
- El-Zant A., Shlosman I., Hoffman Y., 2001, ApJ, 560, 636
- Erb D. K., Shapley A. E., Steidel C. C., Pettini M., Adelberger K. L., Hunt M. P., Moorwood A. F. M., Cuby J.-G., 2003, ApJ, 591, 110
- Erb D. K., Steidel C. C., Shapley A. E., Pettini M., Adelberger K. L., 2004, ApJ, 612, 122
- Franx M. et al., 2003, ApJ 587, L79
- Giavalisco M., Dickinson M., 2001, ApJ, 550, 177
- Lacey C., Cole S., 1993, MNRAS, 262, 627
- Marleau F. R., Simard L., 1998, ApJ, 507, 585
- Mo H. J., Mao S., White S. D. M., 1998, MNRAS, 295, 319
- Mo H. J., Mao S., White S. D. M., 1999, MNRAS, 304, 175
- Navarro J. F., Frenk C. S., White S. D. M., 1997, ApJ, 490, 493
- Pettini M., Shapley A. E., Steidel C. C., Cuby J.-G., Dickinson M., Moorwood A. F. M., Adelberger K. L., Giavalisco M., 2001, ApJ, 554, 981
- Primack J. R., Wechsler R. H., Somerville R. S., 2003, in Bender R. & Renzini A., eds. The Mass of Galaxies at Low and High Redshift. Proceedings of the ESO Workshop held in Venice, October 2001
- Shapley A. E., Steidel C. C., Adelberger K. L., Dickinson M., Giavalisco M., Pettini M., 2001, ApJ, 562, 95
- Shapley A. E., Steidel C. C., Pettini M., Adelberger K. L., 2003, ApJ, 588, 65
- Smail I., Ivison R. J., Blain A. W., 1997, ApJ, 490, L5
- Somerville R. S., Primack J. R., Faber S. M., 2001, MNRAS, 320, 504
- Steidel C. C., Hamilton D., 1993, AJ, 105, 2017
- Steidel C. C., Pettini M., Hamilton D., 1995, AJ, 110, 2519
- Weatherley S. J., Warren S. J., 2003, MNRAS, 345, L29
- Wechsler R. H., Somerville R. S., Bullock J. S., Kolatt T. S., Primack J. R., Blumenthal G. R., Dekel A., 2001, ApJ, 554, 85

This paper has been typeset from a $\text{\TeX}/\text{\LaTeX}$ file prepared by the author.